

Monitoring the effects of weed management strategies on tree canopy structure and growth using UAV-LiDAR in a young almond orchard

Tamir Caras^a, Ran Nisim Lati^b, Doron Holland^c, Vladislav Moshe Dubinin^{a,d}, Kamel Hatib^c, Itay Shulner^b, Ohaliav Keiesar^e, Guy Liddor^e, Tarin Paz-Kagan^{a,*}

^a French Associates Institute for Agriculture and Biotechnology of Dryland, The Jacob Blaustein Institutes for Desert Research, Ben-Gurion University of the Negev, Sede Boqer Campus, 8499000, Israel

^b Department of Weed Research and Plant Pathology, Agricultural Research Organization, Neve Ya'ar Research Center, Israel

^c Unit of Fruit Tree Sciences, Agricultural Research Organization, Neve Ya'ar Research Center, Israel

^d Earth and Planetary Sciences Department, Weizmann Institute, Rehovot, Israel

^e The Department of Sensing, Information and Mechanization Engineering, Institute of Agricultural Engineering, Agricultural Research Organization, Volcani Center, Israel



ARTICLE INFO

Keywords:

Integrated weed management (IWM)

Leaf density

Gap Fraction Profile (GFP)

Canopy volume

Yield assessment

Structural parameters

Herbicide

Almond orchard

UAV - LiDAR

ABSTRACT

The primary objective of this study was to assess the potential effect of integrated weed management (IWM) on canopy structure and growth in a young almond orchard using unmanned aerial vehicle (UAV) LiDAR point cloud data. The experiment took place in the Neve Ya'ar Model Farm, with four IWM strategies tested: (1) standard herbicide, (2) physical-mechanical, (3) cover crops, and (4) integrated management combining herbicide and mowing. One pre-treatment sessions in 2019 and two experiment sessions in 2020–2021 were conducted. During these three experimental sessions, manual measurements, including trunk diameter (TD), were taken for all trees in the orchard. Six canopy growth parameters (e.g., tree height and volume), and functionality parameters (e.g., leaf density, gap fraction profile (GFP) and entropy) were calculated for individual trees using UAV-LiDAR data and were compared to manual measurement (i.e., TD). The results indicated that the herbicide treatment enabled effectively maintained weed coverage at approximately 5–10 % throughout the experiment, demonstrating successful control over weed growth. In contrast, the integrated weed management strategy yielded the highest weed cover (~50 %). With the view of replacing ground manual measurements with UAV-LiDAR-derived measurements, we explored the relationships between TD and UAV-LiDAR-derived volume and GFP. The relationships between TD and GFP were with R^2 values of 0.43 and 0.57 for 2021, respectively. The relationship between GFP and volume showed an R^2 value of 0.65 for both years. We observed significant differences between IWM for TD, volume, and GFP in both years, indicating on higher tree development in the herbicide and integrated management treatments. The standard herbicide-based management yielded the highest crop yield, while the cover crop strategy yielded the lowest per plot. Finally, random forest (RF) model was used to identify key factors that significantly influence tree volume, TD, and GFP. The RF results showed that IWM explained about 30 % of tree structural changes, while the rest were attributed to environmental factors (i.e., topographical and climatic). The RF model R^2 values ranged between 0.79 and 0.86, representing the topographical and climatic effects on tree structural parameters and growth, reflecting the natural field variability. Our study designed and successfully implemented a framework for estimating canopy characterization in young almond orchards subjected to varied IWM treatments. Ensuring the precise calibration of the LiDAR system and validating data, especially in complex canopy structures, can be challenging since the accuracy of ground-truth data has its errors. For future study, the fusion of LiDAR data with multispectral imagery or terrestrial LiDAR data can be considered, as well as more frequent UAV-LiDAR re-visits, offering insights into phenological states and higher resolution of canopy characteristics in orchards. This research enhances our understanding of the advantages and challenges of using UAV-LiDAR point cloud data analysis to assess the impact of IWM on young almond tree growth.

* Corresponding author.

E-mail address: tarin@bgu.ac.il (T. Paz-Kagan).

1. Introduction

Precision agriculture (PA) combines information and technologies to improve farming practices based on spatial and temporal variabilities. The data provides additional knowledge to evaluate crop health and productivity to improve agricultural management decision-making (Westwood et al., 2018; Zhang et al., 2021; Zhao and Popescu, 2020). One such decision is weed management in orchards, where successful management results in healthier trees, better development, and higher yield (e.g., Bajwa et al., 2015; Gianessi and Reignier, 2007; Lati et al., 2021). Herbicides constitute the principal weed management method used in most fruit orchards in industrialized countries (Fennimore and Doohan, 2008). Herbicides are considered a highly effective treatment, requiring minimal human labor and time investments while ensuring optimal fruit yield (Moretti et al., 2021). Nevertheless, the adverse health effects associated with herbicide use have become widely known, leading to increased demands for regulations and enforcement of relevant laws (Westwood et al., 2018). Various herbicides have thus been or will be, subject to strict regulatory measures that limit or prohibit their use (Bajwa et al., 2015), and such restrictions will have local and immediate knock-down effects on yield. Therefore, the economic profitability of various fruit crops is expected to affect global food security (Jabran and Chauhan, 2018). As a result, stakeholders are more motivated to introduce non-chemical weed control tools and develop integrated weed management (IWM) approaches that will help maintain crop health and productivity. Exploiting these alternative weed control methods can mitigate the current over-reliance on herbicides (Lati et al., 2021).

For orchards, several alternative, non-chemical weed control approaches have been suggested (e.g., Granatstein et al., 2010), including mechanical (e.g., cultivation), physical (e.g., flaming), and ground cover strategies (e.g., mulching). Combining these approaches would facilitate an IWM strategy that should affect a reduced reliance on herbicide-based weed control to support more targeted herbicide application. While IWM strategies may be operationally applicable, their efficacy is affected by various environmental and management parameters that can limit their operation (Melander et al., 2005). Moreover, alternating between weed control methods may affect tree performance and yields (Guerra and Steenwerth, 2012), and as such, the choice between alternative weed control strategies must be carefully considered. Therefore, one of the current knowledge gaps lies in the limited understanding of how various weed management strategies impact tree development and overall orchard performance. This knowledge gap is particularly relevant for young trees, which possess less developed root systems and are more vulnerable to competition from weeds (Bond and Grundy, 2001; Mechergui et al., 2021). Moreover, there is a need for a dependable method that can accurately estimate and predict the effect of IWM on current tree development in terms of overall tree health, growth status, functionality, and, therefore, potential yield.

Estimates of tree canopy geometrical and morphological traits can be calculated using a physical or functional approach (Janick, 2006; Lee and Ehsani, 2009; Rosell and Sanz, 2012; Torres-Sánchez et al., 2018). The physical approach calculates canopy structural dimensions, such as volume or height, as studies have shown a linear correlation between the tree's geometrical parameters and yield (Hill et al., 1987; Underwood et al., 2016). Canopy functionality, such as Gap Fraction Profile (GFP), is based on allometric methods using three-dimensional (3D) models and is related to the canopy's photosynthetic activity and radiation (PAR). In turn, the extent of light capture at the tree level is directly linked to the maximal yield and profit potential (Zarate-Valdez et al., 2015). The combined physical-functional approach exploits biophysical parameters and size to estimate the tree canopy functionality traits (Bellvert et al., 2021; Zhang et al., 2019; Zhao et al., 2017). Traditional canopy trait estimates are inherently inaccurate, partly due to the inaccuracies of manual measurement techniques (West, 2009). Additionally, these estimates assume simplistic geometric models (such as cones,

hemispheres, or ovoids), which fail to capture the natural irregularities in the shapes of trees (Torres-Sánchez et al., 2018). Therefore, there is a need for a more accurate alternative and less labor-intensive method for estimating tree canopy size (Fan et al., 2020; Gao et al., 2021; Kamoske et al., 2019). In this context, remote sensing (RS) based on 3D models emerges as a prominent non-destructive alternative for collecting structural data (Fan et al., 2020; Tian et al., 2021; Yin and Wang, 2019). This method typically utilizes active sensors and requires minimal fieldwork, making it an efficient and reliable option for assessing tree structure parameters.

Several well-established RS methods are available for constructing 3D models, including structure formation (SfM) photogrammetry and LiDAR technologies (Beniston et al., 2016; Rosell and Sanz, 2012; Zhang et al., 2021). LiDAR, a relatively recent addition to the suite of UAVs sensors used in PA, has demonstrated its potential for accurately mapping and measuring various structural traits of tree canopies (e.g., Rosell and Sanz, 2012; Torres-Sánchez et al., 2018; Zhao et al., 2020). LiDAR systems are based on active sensors that emit multiple high-frequency laser pulses at the target object, measuring the time it takes for the laser pulse to travel to the object and back to the sensor. Among the various RS technologies mentioned above, LiDAR seems particularly well-suited to evaluating tree structures and supporting the implementation of IWM. Indeed, mounting the sensor on board a UAV enables mapping hundreds of points per square meter to obtain the final output, a point cloud. The resulting data-rich point cloud allows exploring site-specific tree canopy parameters via dedicated algorithms. With this in mind, although LiDAR is widely used in forestry applications (e.g., Asner et al., 2003; Jarron et al., 2020; Underwood et al., 2016; Verma et al., 2016), the technology has enjoyed only limited use in orchard crop management. In contrast to the data collected by passive sensors, such as spectral data, LiDAR, an active sensor, has some fundamental advantages: (1) LiDAR operation is independent of light conditions and climate conditions, and (2) it directly measures canopy structural traits and architecture.

Zhu et al. (2021) suggest two approaches for tree volume estimation: the geometric shape approximation and the computational geometric approach. While the former usually assumes a spherical or oval tree canopy shape (Rosell and Sanz, 2012; Zhu et al., 2021), computational approach models, in contrast, rely on point cloud-derived data. Without the assumption of canopy shape, they can account for irregularities in the tree canopy, such as growth gaps (Volume added by inter-brachial spaces) and extensions of branches (Rosell and Sanz, 2012; Underwood et al., 2016; Zhu et al., 2008, 2021). Canopy volume measurement can be done by converting the LiDAR-generated point cloud to a systematically and geospatially ordered point cloud. Wherein all of the points within a fixed-size cube are summarized into a single value per category, it is suggested that the volumetric pixel, or voxel, is used (Zhao and Popescu, 2020; Zhu et al., 2020, 2021). Voxel spatial resolution is analogous to image pixel size and tightly linked to object size and complexity. The geometric shape approximation and computational geometric approaches have thus markedly improved the analysis of the point cloud data of tree structures collected from LiDAR systems.

The current study deliberately focused on young almond orchards, specifically those 3–4 years old, despite the potential limitations of their high yield instability and unpredictability. This decision was based on recognizing that young trees are more vulnerable to weed management impact than mature trees (Mia et al., 2020). Young trees are more susceptible to competition from weeds, and the effects of IWM applications during their early development stages can significantly impact their future growth and survival, whereas these effects tend to diminish substantially in mature trees (Gianessi and Reignier, 2007; Moretti et al., 2021). Weed management, therefore, plays a vital role in the success of fruit crop tree endeavors and the overall profitability of orchards (Belding et al., 2004). The potential impacts of these effects are particularly heightened in young orchards, which refer to the first four years after plantation. During this critical establishment phase, adequate weed

control is essential to ensure the development of a healthy orchard and optimize future fruit production (Mia et al., 2020).

We aimed to link weed management practices, tree growth, and yield in a young almond (*Prunus dulcis* (Mill.) D. A. Webb) orchard using structural parameters obtained from UAV-LiDAR. Like other fruit crop trees, almonds are an intensively managed, high-economic-value crop. Almond tree competition with weeds for resources such as water and nutrients affects tree development and growth (Belding et al., 2004), potentially reducing crop yield, quality, and quantity (Brunharo et al., 2020). Thus, our specific objectives were: (1) to evaluate tree growth parameters and monitor their changes under different weed control strategies at the tree and regional scale (i.e., orchard) in 2019–2021, (2) to develop a methodology using UAV-LiDAR for monitoring tree structure parameters, including tree height, volume, and GFP, in a young almond orchard, (3) to quantify the relative influence of weed management practices and environmental factors on the change in growth parameters, and (4) to examine the relationship between weed control strategies and overall yield at the plot level.

2. Methods

2.1. Study site

To answer the study objectives, the UAV-LiDAR was used to monitor young almond tree development under different weed control strategies in a controlled experiment in the Neve Ya'ar Model farm. The study was carried out in an experimental orchard measuring 1.6 ha and with a 5 % slope, where young almond trees were planted in January 2019 (Fig. 1);

(Figure S.1). The orchard is located at the Neve Ya'ar Research Center in the Jezreel Valley, Israel (32.70° N, 35.18° E). The studied almond trees were the self-pollinating cultivar 'Matan' grafted on GF.677 rootstock (Holland et al., 2016). Trees were planted 17 to a row (every 6 m) in 22 rows spaced 7 m apart (with 374 trees overall). Details of the irrigation treatments can be found in Table S.1, while the fertilization regime is provided in Table S.2. It is important to note that the natural variability in commercial orchards primarily arises from factors that cannot be controlled, such as elevation, slope and aspect, and other site-specific natural variability. The soil in the orchard is uniform, with a noticeable elevation gradient toward the river channel dry most of the year (Figure S.1).

2.2. Experimental design of the weed treatment

Four weed control strategies were tested in an experiment run from October 2019 to October 2021, encompassing two growing seasons: October 2019 to October 2020 (first season) and October 2020 to October 2021 (second season, Figure S.2). The weed control strategies included (1) standard herbicide, (2) cover crops, (3) physical-mechanical, and (4) integrated strategy that comprised a combination of herbicide and mowing. Table 1 contains a detailed description of the weed control strategies applied in the experiment, and those are outlined in Fig. 2. The experiment layout is a randomized block design comprising five repetitions for each treatment for a total of 20 plots. Each repetition contained 16 trees arranged in two rows of eight trees.

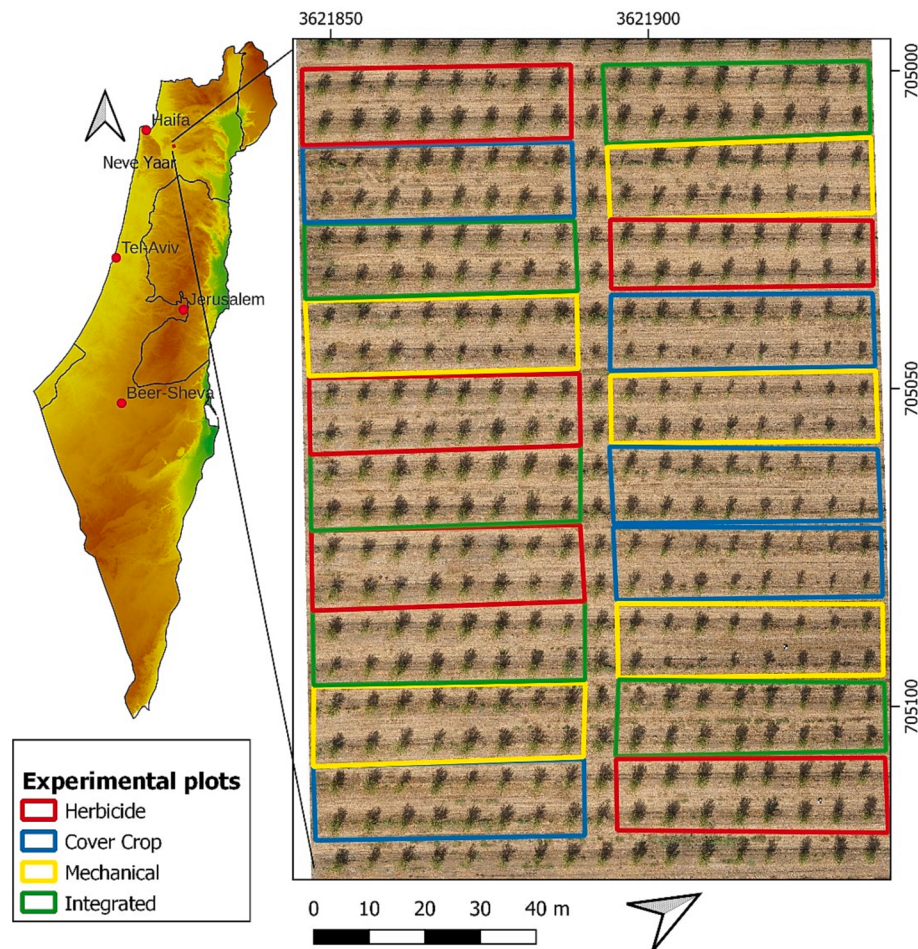


Fig. 1. The study area was an experimental almond orchard at the Neve Ya'ar Research Center in the Jezreel Valley, Israel. The experimental block colors represent the four-weed control/management strategies applied in the orchard.

Table 1

Weed control/management strategies were tested in an experiment from October 2019 to October 2021.

Weed control strategies - Detailed descriptions	
Herbicide	In the first season, trees were young and sensitive. Thus, only post-emergence herbicides were used. Glyphosate at a rate of 480 g ai ha ⁻¹ with glufosinate-ammonium at a rate of 500 g ha ⁻¹ was applied on October 30, 2019, April 4, 2020, June 4, 2020, and September 5, 2020. As trees were more developed in the second season, pre-emergence herbicide could be used. Indaziflam was applied at 75 g a.i. ha ⁻¹ on December 14, 2020, and activated by rain. Herbicides were sprayed using a motorized back sprayer equipped with a 2-m-wide ground spray rod and a Teejet-110015 nozzle (Spraying Systems Co., Wheaton, IL), with a spray volume of 200 L ha ⁻¹ .
Mechanical	Flaming combined with a finger weeder – Flaming was carried out using an un-shielded Red Dragon three-burner system equipped with one liquid-phase torch (LT 6 × 18 super torch; Flame Engineering Inc., LaCrosse, KS, USA) and two smaller torches (LT 1 1/2 × 6) connected to 2019 a 500-L LPG tank mounted on a cart. The treated area comprised a 1-m wide swath on each side of the tree line at an LPG rate of 60 kg ha ⁻¹ . In the first season, three flaming treatments were applied in the winter (February-April 2020), and three finger weeder treatments were applied in the summer (April-July 2020). Five flaming treatments were used during the second season during the winter (December 2020-April 2021). Two finger weeder treatments were applied during the summer (April-September 2021).
Cover Crops	A combination of oat (<i>Avena sativa</i>), vetch (<i>Vicia sativa</i>), and clover (<i>Trifolium incarnatum</i>) crops were seeded on December 2, 2019, and September 12, 2020, at the rate of 10 kg ha ⁻¹ . Beginning on 22 and 4 April 2020 and 2021, respectively, the cover crops were mowed five times during the year-long study.
Integrated	This treatment included herbicide application on the tree line (0.5 m from tree sides) and mowing on the rest of the area (1.5 m from tree sides). In the first year, the tree line area was sprayed with glyphosate and glufosinate-ammonium at the timing and rates described in the herbicide section. In the second year, the tree line area was sprayed with Indaziflam. Herbicides were sprayed using a 0.5 m wide ground spray rod on the tree line, and weeds at the 1 m width were mowed three and five times in the first and second seasons, respectively.

2.3. Ground measurements and yield assessments

In the first season, weed control was estimated three times by counting the number of weeds in four 0.25 m² quadrats randomly placed in each treatment. In the second season, weed control was visually assessed monthly by ground cover estimations for ten months. The ground crown mensuration parameters included trunk diameter (TD). The standard TD measurement was used here because it was shown to represent almond growth and to be related to different structural parameters and almond yields. It also represented relatively accurate other growth parameters (Rojo et al., 2014). The TD of each tree in the orchard was manually and directly measured in the pre-treatment in October 2019 and at the end of the first and second sessions of the experiment on 25 and 28 December 2020 and 2021, respectively. The TD was measured on the tree's trunk 50 cm above the soil surface. For yield evaluation, almonds were manually harvested from all trees and were pooled by repetition plots (n = 20), and their gross weight was measured. Harvest was conducted on 8 and 15 August 2021 (with about 700–1000 Kg ha⁻¹). The time frame of the experiment application is detailed in Figure S.2.

2.4. UAV LiDAR data acquisition

Two UAV flights were executed approximately one year apart (September 30, 2020, and October 11, 2021) at the end of the growing season when almond trees typically carry almost full leaf cover. The flights were conducted during midday, specifically between 10:30 and 13:00 local time (GMT + 2), under clear sky conditions. The UAVs operated at a speed of 3.5 m per second and maintained an altitude of 30 m above the ground. The captured images had a spatial resolution of 5.5 cm per pixel. The UAV platforms were equipped with various sensors, such as high-resolution LiDAR sensors, multispectral cameras with thermal band detection capability, and a high-resolution RGB camera. The data were acquired using a Matrice pro-600 UAV outfitted with a RIEGL miniVUX-1UAV laser scanner designed specifically to be integrated with UAV platforms and fused with a Sony alpha 6000 RGB



Fig. 2. Experimental orchard and the experimental setup for the weed management strategies. (A) Standard herbicide, (B) cover crops, (C) physical-mechanical, and (D) integrated, a combination of herbicide and mowing.

camera. The LiDAR data pre-processing comprised of importing and adjusting flight trajectory, data cleansing, geo-rectification, and finally exporting the data in LAS format was undertaken using RIEGL software (Applanix POSPAC, Riegl RiProcess, Riegl RiPrecision (Brede et al., 2017). All point cloud processing and analysis were conducted using specially scripted code in R language that utilized dedicated LiDAR libraries like LidR (Roussel et al., 2020) and Rlidar (Silva et al., 2016). The LiDAR analysis workflow consists of four main stages (Fig. 3): (1) construction of a LiDAR-based model for estimating tree-level structural parameters between growing seasons; (2) comparison of the structural parameters of the modeled tree between years and identification of correlations between the LiDAR structural parameters and the TD measurements that were manually collected on the ground; (3) estimation of the effects of the weed control strategies on tree structural parameters; and (4) testing of the relations between tree structural parameters, the experimental weed control classes and yield. The outputs derived from this step were spatial and temporal structural parameters for each weed control experiment. Finally, we applied a random forest (RF) model to identify key factors that significantly influence changes in tree volume, TD, and GFP.

2.5. Analysis of point cloud derived from LiDAR data

Several analytical steps were undertaken for the LiDAR canopy structure parameters. After importing the raw data from LiDAR into a point cloud format, a pre-processing workflow (e.g., clipping, cleaning, and reclassification) was conducted. All points classed as “ground” were converted to a height of 0 during normalization. From this base, the tree top canopy height was subtracted (thereby omitting the topography variation in the cloud data). Tree canopy height (TCH) and the digital elevation model (DEM) were used to generate the canopy height model (CHM), which separates trees from other points in the point cloud (namely, points classified as ground and low vegetation) (Roussel et al., 2020; Silva et al., 2016; Yang et al., 2020).

The next step – segmentation- canopy separation- is accomplished using a watershed algorithm (e.g., Burt et al., 2019; Torres-Sánchez et al., 2018; Zhao et al., 2020). This algorithm, implemented within the lidR library (Roussel et al., 2020), relies on the point cloud and the CHM as input. It considers optimization factors such as the distance between trees, tree size, and a sensitivity threshold to prevent potential overlapping cases and assigns a unique ID number to each tree. Only a few instances of overlapping trees were recorded due to the young age of these trees (2–3 years). The next step in canopy parameter calculations was summarizing point cloud data into voxels, three-dimensional pixels with dimensions of 0.25 m and a volume of 0.015 m³. This voxel size was carefully chosen to strike the optimal balance between computing power, data complexity, and the specific characteristics of the young tree canopy. The voxel dataset enabled us to explore the data in columns or height-stratified layers, facilitating precise procedures such as density and volume calculations. The voxels below one meter were filtered out from the dataset, leaving only those that contained trees (also omitting voxels positioned in gaps between trees). Tree data was then exported to a database for statistical analysis per tree ID.

2.6. Canopy structural and functional parameter calculations

Several key structural parameters were extracted from the workflow described above, including tree volume and height. Tree volume was calculated by summing up all voxels containing points in the canopy. This volume estimation is accurate, considering that a voxel size of 0.25 m per voxel is fine enough to omit all within-canopy gaps from volume estimates. Tree height was measured as the TCH point in the canopy. Additionally, four canopy functional parameters were calculated: Leaf Area Density (LAD), Gap Fraction (GFP), Vegetation Cover Index (VCI) (Ewijk et al., 2011), and Entropy (Roussel et al., 2020; Zhao and Popescu, 2020). LAD and GFP represent aspects of canopy density, such as Leaf Area Index (LAI), which is often correlated with photosynthesis efficiency, productivity, and yield (Bouvier et al., 2015). LAD is

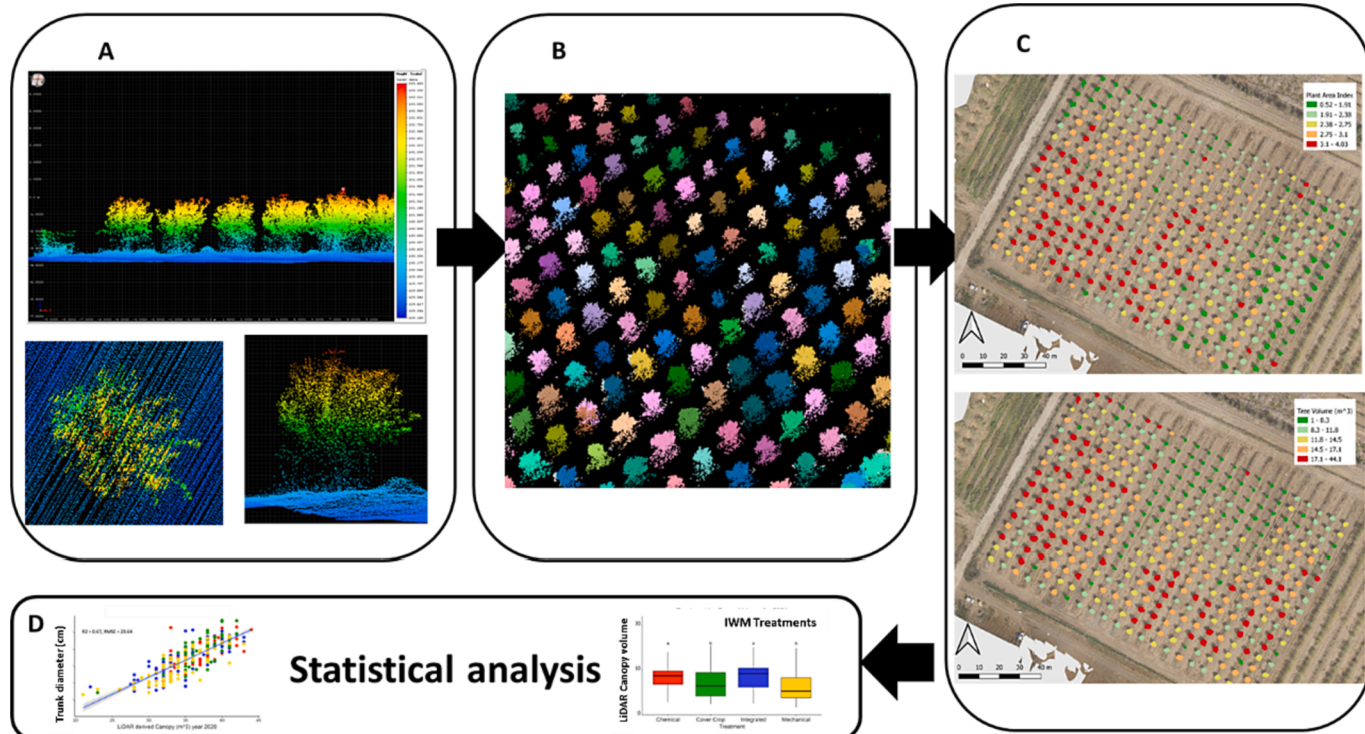


Fig. 3. LiDAR data collection and analysis. (A) Point cloud processing. (B) height normalization and canopy segmentation. (C) extraction from the point cloud of tree volume, and gap fraction profile (GFP). (D) Statistical analysis comprised tests of the differences between integrated weed management (IWM) and estimates of ground measurements.

calculated from the GFP voxel value by applying the Beer-Lambert law, adjusting values based on the estimated canopy shape. Essentially, GFP measures light interception (and thereby absorption) by a voxel, while LAD estimates leaf density irrespective of its utility in light absorption. In this study, we chose GFP over LAD because it is a better representative of canopy functionality and a better predictor of productivity, especially in almond trees where the canopy is loosely arranged (Casanova-Gascón et al., 2019). VCI and Entropy are both measurements of shape and structural variability (Ewijk et al., 2011). Open-structure canopies will get a higher score for Entropy and VCI, thus well correlated with GFP. Therefore, this study further analyzes the parameters of volume and GFP as key representatives of canopy structure and functionality.

2.7. Statistical analysis

The statistical analysis included several steps to test the relations between weed control management and the canopy structural parameters. Eight trees were excluded from the database as they were severely damaged between 2020 and 2021, reducing the number of trees from 320 to 312 in the analysis. A conservative approach was also used, employing the median absolute deviation (MAD) to remove 2.5 % of residuals at both ends of the distribution for each variable before conducting each statistical test. At this stage, 15 trees were removed, resulting in a minimum of 297 trees remaining for analysis. The correlations between all the described canopy geometry parameters extracted from the LiDAR data and those manually measured on the ground (i.e., TD) were explored using a predictive power score (PPS, Sharma, 2020; Wetschoreck et al., 2020), and in specific cases, standard regression tests were used. Four statistical approaches were explored: (1) the linear and nonlinear correlations between all structural and functional canopy parameters extracted from the LiDAR data and those measured manually on the ground (i.e., TD); (2) the effects of the weed treatment experiment on selected tree canopy geometries; (3) the correlation between tree geometry, experimental treatment, and yield. For the latter, because the yield was collected per plot, canopy geometry, and TD were averaged per plot; (4) RF model to identify key factors (i.e., IWM and environmental factors) significantly influencing tree volume, TD, and GFP change.

A predictive power score (PPS) matrix (Levi et al., 2022; Sharma, 2020; Wetschoreck et al., 2020) was used to test the nonlinear correlation for all LiDAR-derived canopy geometries and the on-ground manually measured TD. Additionally, it allows for different scoring for cases that exhibit pairing asymmetry (i.e., $X \sim Y \neq Y \sim X$) and data directionality between tested pairs. The score is considered conservative because it merges accuracy (i.e., elements analogous to root mean square error (RMSE)) with a correlation estimate (analogous to R^2). The PPS approach was used here as an overview indicator to evaluate the tree growth parameter's nonlinear relations. In addition to the PPS, linear correlations were calculated for selected pairs of tree growth parameters (volume, GFP, and TD) to obtain the adjusted R^2 and RMSE. In most cases, nonparametric statistical tests were used because data were not always normally distributed and to increase their robustness. For the boxplots, a Kruskal-Wallis one-way analysis of variance test for significance and a Tukey test (linear model post hoc test) were used to assess the difference within and between the experimental weed control treatments. Unlike the per-tree dataset, the per-plot correlation focused on the relationship between tree geometries (averaged per plot), treatment, and yield (sum per plot).

2.8. Random forest model

IWM treatments were implemented to ensure uniformity while maintaining all management factors (e.g., irrigation, fertigation, tree type, age) as consistently as possible. Nonetheless, certain uncontrollable environmental factors also influence tree development. These factors might exhibit non-uniformity, such as topography (with a subtle slope

from north to south), water availability, soil nutrient content, and microclimate variations. Consequently, their measurement effects are important to consider. Given this context, our framework's final step utilized the RF algorithm to assess the partial contributions of environmental explanatory factors and the IWM to tree geometry. The RF algorithm, as described by Rodriguez-Galiano et al. (2012), is a nonparametric statistical method. It gauges the relative significance of tested explanatory variables observed in metrics like tree volume, GFP, and TD. We initially selected six environmental parameters and IWM to analyze tree development, representing them as spatial layers. Using the GRASS GIS toolboxes, we derived terrain features like slope, aspect, and elevation from LiDAR data DEM. We computed distances from spatial-environmental features like streams and adjacent fields by applying the Euclidean distance algorithm to a DEM-based stream network using the SAGA toolbox within QGIS. We employed label encoding for the categorical variable, IWM, as it was input as a factor in the RF model. To eliminate model redundancy and collinearity, we created a correlation matrix among all the environmental parameters, ensuring the variables selected were independent. Owing to the correlation between slope, aspect, and DEM with "distance from streams," we chose the latter to represent the topographical factors (Table S.4). As a result, two non-correlated environmental parameters, alongside the IWM categories, were used as input for the RF model, namely the distance from streams and adjacent fields. Our analysis established meta-variables, such as decision-tree depth and learning rate, and incorporated 500 decision trees (Ai et al., 2014). The dependent variables in the RF models were tree geometries (TD for 2019–2021, GFP for 2020–2021, volume for 2020–2021), while the predictors included IWM, distance from streams, and adjacent fields using the Euclidean distance function, with a total of seven RF models tested. We performed the RF analysis using R's machine-learning platform in the caret library (Kuhn, 2008).

3. Results

3.1. Weed control cover

The IWM treatments significantly influenced weed density, but there were some differences between the two seasons (Fig. 4). In 2020, when the trees were younger, only post-emergence herbicides were applied, resulting in suboptimal weed control, and weed cover was approximately 15 %. These results were similar to the cover crop treatment, which had around 10 % weed cover. The integrated and mechanical-physical treatments were less effective, with weed cover estimations exceeding 30 %. In 2021, using pre-emergence herbicides, the herbicide treatment showed favorable control results, and weed coverage remained at around 5 % throughout the experiment. The plots where an integrated weed control method was tested showed the highest weed coverage values, i.e., approximately 50 %, indicating the low efficacy of this treatment. The results of the cover crop treatment did not differ significantly from those observed with the herbicide treatment, under which weed coverage was approximately 15 % throughout the year, with significant differences between dates. Table S.3 includes all the detailed results of weed cover responses and the species detected in response to the IWM different treatments for 2020 and 2021, respectively.

3.2. Tree dimensions comparisons

Fig. 5 displays the PPS matrix for the structural attributes in 2020 and 2021. As introduced in the statistical analysis section. PPS values above 0.5 signify a strong nonlinear relationship (Levi et al., 2022; Sharma, 2020; Wetschoreck et al., 2020). In our score matrix, the highest values reached 0.83 for parameter pairs like GFP and height. VCI also showed a high correlation with height, GFP, and volume. However, we selected GFP and canopy volume from the LiDAR-derived parameters primarily because they offer the most meaningful, practical, and

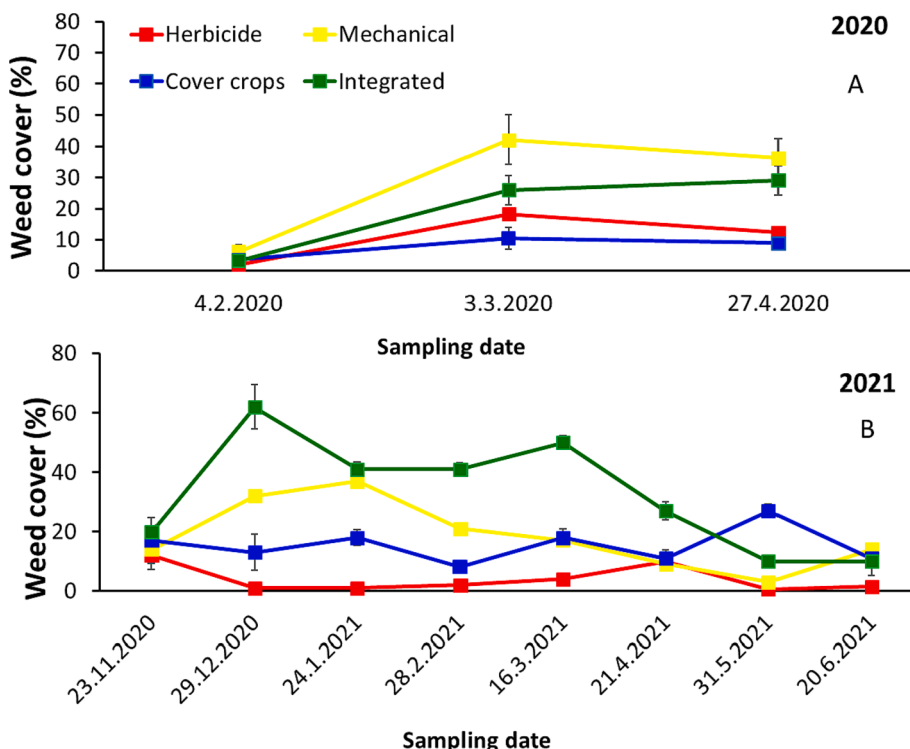


Fig. 4. (A) The average values of weed cover for 2020 and (B) 2021 for the four treatments. The weed control treatments include (red) standard herbicide, (blue) cover crops, (yellow) physical-mechanical, and (green) integrated, a combination of herbicide and mowing. (For interpretation of the references to color in this figure legend, the reader is referred to the web version of this article.)

standardized parameters while addressing the structural and functional tree parameters for subsequent analysis. With this in mind, our study aimed to determine if LiDAR-collected data could correlate to TD manually collected ground data. Thus, we emphasized the nonlinear correlation between GFP, canopy volume, and TD (Fig. 5). TD was the sole parameter present before the initiation of the weed control experiment in 2019. As expected, the PPS values with all structural parameters in subsequent years are notably low (below 0.01). TD's 2020 PPS with other 2020 geometric values ranged from 0.1 to 0.26; these values increased in 2021 (0.15–0.33). Specifically, TD's 2020 PPS with canopy volume and GFP were lower in 2020 (PPS scores of 0.13 and 0.21, respectively) than their 2021 values (PPS scores of 0.23 and 0.31, respectively). Figure 6 illustrates the linear correlations (R^2) among our focal parameters, namely TD, canopy volume, and GFP. The linear correlation of TD to canopy volume (R^2 0.28 to 0.43 for 2020 and 2021, respectively) and GFP (R^2 0.48 to 0.57 for 2020 and 2021) showed stronger relations in both PPS and linear correlations 2021 than in 2020. However, the linear correlation between GFP and canopy volume remained consistent for both years, with an R^2 value of 0.65. The relatively good correlation between ground-collected TD and LiDAR-derived variables suggests that the former can replace the latter.

The weed control treatment scheme significantly affected tree volume, GFP, and TD (Fig. 7). The within-treatment size distributions of canopy geometry are affected by treatment and increase from 2020 to 2021. TD trend stretches over the three years recorded is particularly evident that before experimental treatment started, there were no significant differences between the canopy geometries. Tree geometries seem to be divided into two treatment groups. Typically, there were no significant differences between the herbicide and integrated treatments, and cover crop and mechanical treatments seem to have similar effects. The integrated and herbicide weed control strategies promoted larger tree geometries, while trees exposed to the mechanical and crop cover treatments generally exhibited smaller geometries.

We tested the effect of the integrated weed management treatments

on GFP, volume, and TD as structural attributes of trees for the years 2020–2021 (Table 2). When testing the effects of the change between the year's, significant differences were shown in TD, volume, and GFP for the herbicide treatment, the volume and GFP for the IWM.

3.3. Spatial distribution of geometric parameters

When mapping tree geometry values on an orchard scale, patterns emerge that do not strictly align with the experimental design. An irregular spatial distribution with increasing magnitude along the northeast-to-southwest axis is visible for the three tested tree geometry parameters (volume, GFP, and TD), as depicted in Figs. 8 and 9. Analysis of the TD maps reveals that the distribution patterns of tree size underwent marked changes between 2019 and 2020, suggesting that spatially, the effects of the weed control treatments required at least one season to manifest, which increased in the second session (Fig. 8). Additionally, it is interesting to note that the similarity in size distribution indicated by the three tree geometry measurements points to environmental factors responsible for this effect. Fig. 9 illustrates the spatial patterns of tree geometry parameters, including individual measurements of GFP, TD (cm), and tree volume (m^3) for 2020 and 2021. Each map utilizes a distinct color scale to represent the spatial variation of the corresponding tree structure attribute. As the observed trend cannot be solely attributed to weed control treatments, it is likely influenced by other environmental factors not controlled in the current study. To explore these factors, we employed RF spatial analysis to isolate or quantify their effects.

As described in the methods, six different environmental factors were initially tested, but only two factors remained to be tested in the RF model: distance from the stream and the nearby crop field. As indicated in Table S.4, the distance from the stream was found to be correlated with all topographical parameters (elevation, slope, and aspect). Therefore, the three explanatory variables selected for the RF analysis include the distance from the streams, the adjacent field, and the IWM

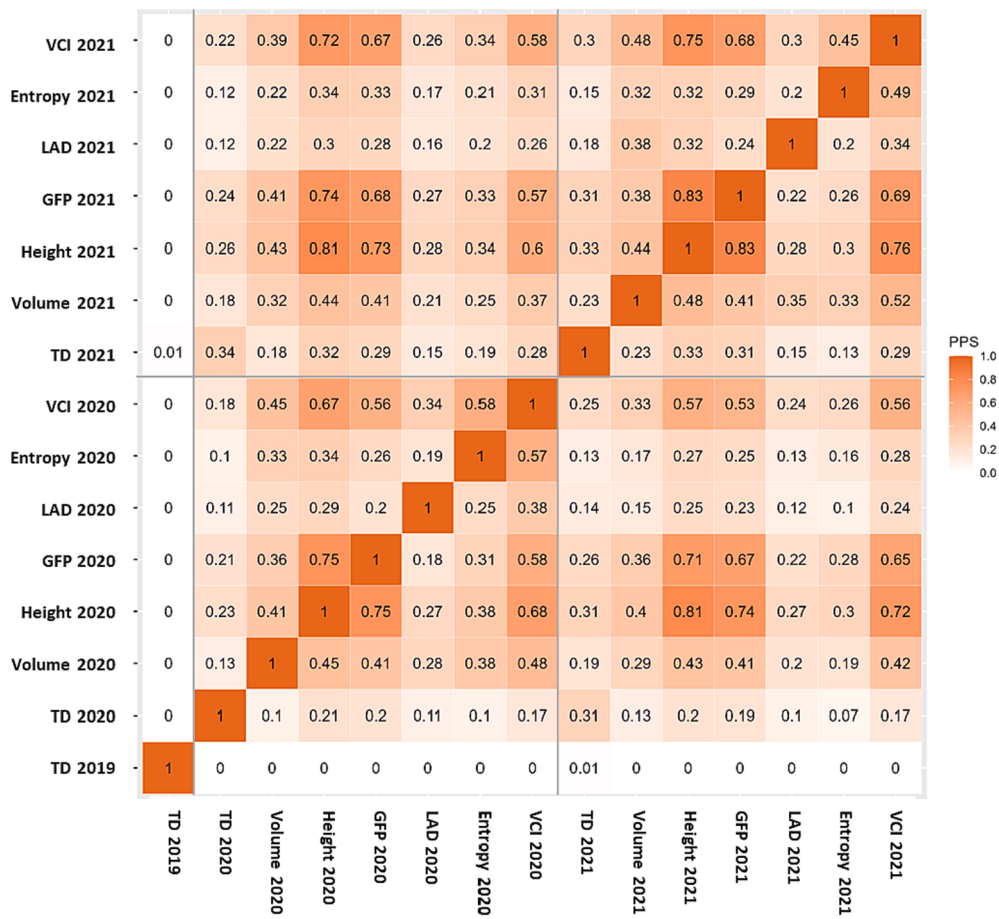


Fig. 5. Predictive Power Score (PPS) matrix for per tree structural attributes. The PPS values that are above 0.5 suggest a strong nonlinear relationship. VCI - Vegetation Cover Index; LAD- Leaf Area Density; GFP - Gap Fraction Profile; Entropy; TD- Trunk diameter.

treatments (Figure S.1). The results of the seven RF models for the three parameters (TD, GFP, and volume) in the sampling years are presented in Fig. 10. The analysis aimed to quantify the partial contribution of the three explaining variables, suggesting that only one-third of the size distribution in the orchard can be attributed to the IWM treatment. At the same time, the two spatial factors equally influenced size distribution. The fact that TD in 2019 was not affected by weed control treatment (before it was implemented) seems to validate these findings. Table S.5 presents the results of all the RF models, including their relative influence, sum of importance, and the R^2 for each model. Most of the RF model results show R^2 values ranging between 0.79 and 0.86, indicating a relatively high representation of the parameters affecting tree structure.

3.4. Yield assessments

The yield for 2021 showed significant differences between treatments (Kruskal-Wallis < 0.05 , Fig. 11). The herbicide-treated plots were the most productive (average above 100 kg per plot). Although, the physical-mechanical treatment plots produced significantly less than the herbicide treatment plots (average above 80 Kg per plot). They were slightly (yet significantly) more productive than the cover crop or integrated treatment plot, with no significant differences (average above 70 kg per plot). Therefore, the yield under the herbicide treatment was significantly higher than that obtained with the cover crop or integrated treatment. The yield results for the physical-mechanical treatment did not differ significantly from those of the cover crop or integrated treatment.

4. Discussion

This study aimed to assess the effects of different weed control strategies (i.e., IWM) on three selected structural parameters (i.e., TD, volume, and GFP) and to test the extent to which these parameters are related to yield in an almond orchard. The results show that the estimates of geometrical (i.e., canopy volume) and functional (i.e., GFP) parameters collected with the UAV-LiDAR provided a reliable method to validate the experimental testing of weed treatments. The PPS matrix was used to explore and quantify these correlations (linear and nonlinear) between tree parameters modeled at the tree level (measurements per tree). We chose to focus on two representatives of tree size (volume) and function (GFP), but it is important to note that other growth parameters may be useful in describing the functionality of tree canopy. For example, VCI (Bouvier et al., 2015; Jarron et al., 2020) measures canopy complexity and directly and indirectly influences almond potential productivity (Casanova-Gascón et al., 2019). We found that the effects of weed control treatment on tree geometry parameters may account for 20–30 % of tree canopy development. Although (or maybe because) these are young trees, some of these correlation and explanatory parameters become tighter in the second year, suggesting that the treatment effect is prolonged. The herbicide treatment and the integrated treatment (including herbicide application along the tree line) promoted generally larger tree geometries than those obtained with the mechanical and crop cover treatments. Unfortunately, yield collection was not done per tree, and it is not possible to statistically correlate tree size with productivity at the individual-tree level. Visually, there is an agreement between size parameters and yield except for the mechanical treatment, where yield is higher than expected from its

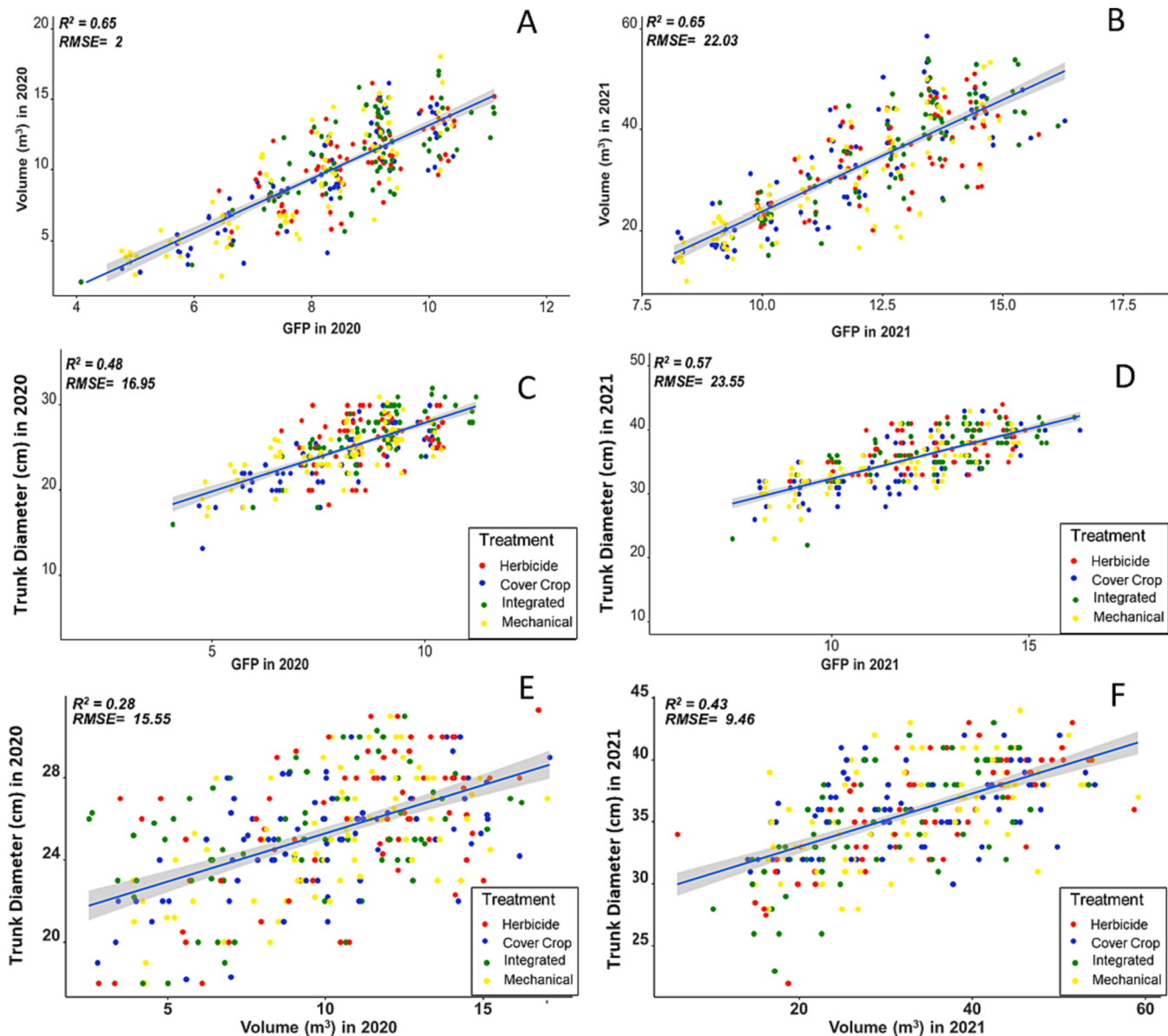


Fig. 6. The correlation among three structural attributes of trees: the Gap Fraction Profile (GFP), canopy volume, and Trunk Diameter (TD) from figures A to F. Data for GFP and Volume are sourced from the UAV-Lidar system, whereas TD measurements are acquired through manual ground-based assessments. Notably, the color of each point represents the corresponding IWM treatment. R^2 and RMSE were calculated for each Figure.

averaged size and similar to the cover crop treatment.

4.1. Tree geometries assessed by LiDAR vs. by on-ground measurements in two years of study

The PPS matrix describes the nonlinear correlations between the data collected on the ground and the data collected with LiDAR. Comparisons between tree geometries in the studied years revealed significant changes in tree volume (approximately double), GFP (20 % increase), and TD (50 % increase) from one year to the next. For example, trees regularly shift their vegetative development and resources toward reproductive efforts (i.e., fruit production), producing fewer and smaller leaves, affecting both canopy volume and GFP estimates. Because the tree imaging in 2021 took place after the almond harvest, we can assume that the point cloud reflects some post-harvest canopy damage, thereby causing an underrepresentation of tree development (particularly volume) for 2021. In retrospect, canopy damage is also very difficult to quantify because it is essentially random per

individual tree and not correlated with the experimental treatments or geospatial parameters (on the orchard scale).

Point clouds can accurately represent complex structures with high within-field variability, such as the almond tree orchard described here. The natural geometry of almond trees consists of widely spaced branches with gaps, which can lead to overestimation of tree volume. This issue may become more significant as the trees continue to grow. To account for this source of potentially growth overestimation error, we set the voxel unit size to 0.25 m, which was determined (based on average leaf and branch sizes) to give the best point aggregation ratio to resolution (Wu et al., 2018). The conversion to voxelized data is calculated as the sum of points or averaged value per voxel. The number of voxels per layer/slice along the height dimension serves as a dynamic unit for estimating the canopy footprint, slice shape, or profile.

The choice to use the GFP algorithm over other leaf density algorithms (namely LAD) is because the latter is normalized per tree. LAD (an improved gap fraction assessment method) gives a better estimate of overall tree density and provides the same weight to voxels in the

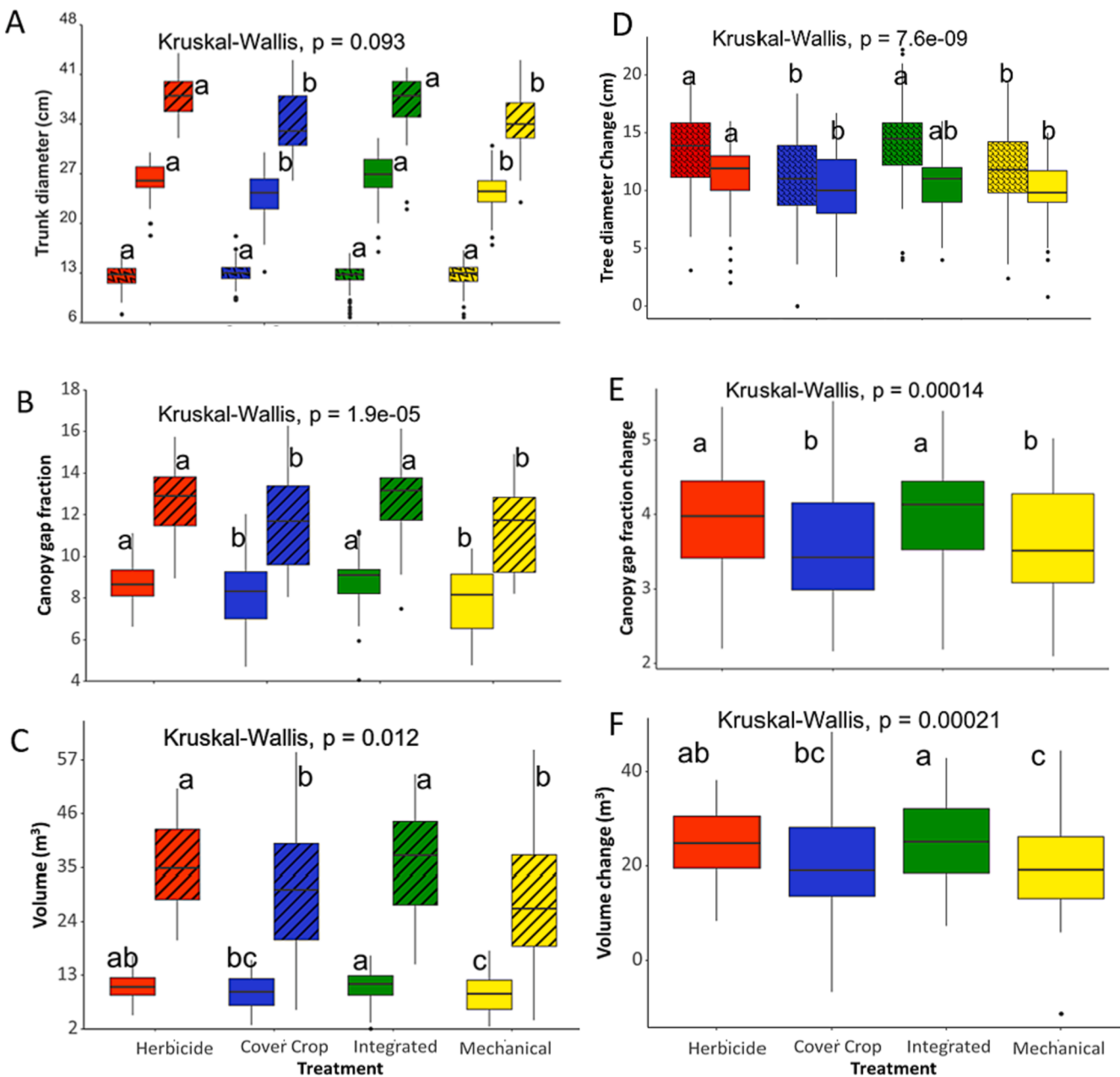


Fig. 7. (A) Statistical differences in Trunk diameter (TD) for integrated weed management (IWM) over three years (2019, 2020, and 2021). (B) Statistical differences in Canopy gap fraction (GFP) in IWM for the years 2020 and 2021. (C) Statistical differences in canopy volume in IWM for the years 2020 and 2021. (D) Statistical differences TD changed between 2019 and 2020 and 2020–2021. (E) Statistical differences in GFP change between the years 2020–2021. (F) Statistical differences in Tree volume change between the years 2020–2021. Kruskal-wallis test results are shown, and the letters represent the post-hoc between-treatment difference. The figure texture highlights the represented years or change (e.g., squiggly fill relates to 2019 data and 2019–2020 change, solid color relates to 2020 or change between 2020 and 2021, and striped texture to 2021).

internal canopy as the ones in the canopy perimeter (Tian et al., 2021). Moreover, this normalization process assumes a canopy shape (oval to spherical), which already adds non-individual-tree-specific bias. Conversely, GFP, essentially doesn't make any assumptions of (or compensation for) canopy shape. Therefore, in a sense, GFP preserves the bias towards the peripheral voxels in almond trees. In turn, the almond canopy inherited open-arrangement provides an improved opportunity for peripheral leaf (better represented by GFP than LAD) participation in photosynthesis (Bouvier et al., 2015) therefore driving yield production. With this in mind, GFP is a preferred yield predictor for almond trees (Casanova-Gascón et al., 2019). Other algorithms for estimating volume and GFP offer alternative approaches that can be tested in future studies (Tian et al., 2021; Zhao and Popescu, 2020; Zhu

et al., 2020). In this respect, the correlation between volume and GFP, as demonstrated in this study provides an opportunity to exploit some volume-GFP discrepancies to signal orchard management that something is affecting leaf density and may require attention. Additional canopy-geometry parameters such as VCI provide potential measurements that, with or without cross-referencing with other parameters, may provide important additional insights. As a PA tool, volume and GFP mapping allow growers to develop site-specific and tree-specific management that adapts to the trees' necessities based on their size and leaf density. In the case of almonds, the optimization, which is based on the tree's architecture, allows for more effective and sustainable yield management while considering IWM-driven spatial variability within the orchards.

Table 2

Statistical differences (SDF) in Trunk diameter (TD, cm), volume (m^3), canopy gap fraction (GFP) response to integrated weed management treatments over a two-study period (2020 and 2021) average and the change, SDF refers to standard deviation.

	Treatment	TD (cm) ± SDF	Volume (m^3) ± SDF	GFP ± SDF	
2020	Cover Crop	23.9 ± 2.9	b 9.6 ± 3.2	bc 1.6	8.07 ± b
	Herbicide	26.1 ± 2.7	a 10.5 ± 2.6	ab 1.0	8.75 ± a
	Integrated	26.9 ± 2.4	a 11.2 ± 2.6	a 1.024	8.86 ± a
	Mechanical	24.3 ± 2.6	b 8.8 ± 3.3	c 1.66	7.75 ± b
2021	Cover Crop	34.1 ± 3.6	b 29.8 ± 10.6	b 2.1	11.6 ± b
	Herbicide	37.4 ± 2.9	a 35.3 ± 8.3	a 1.6	12.6 ± a
	Integrated	37.3 ± 2.9	a 37.3 ± 9.5	a 1.8	12.8 ± a
	Mechanical	34.1 ± 3	b 28.2 ± 9.9	b 2.0	11.3 ± b
Change	Cover Crop	10.1 ± 2.3	b 20.4 ± 8.2	bc 0.7	3.53 ± b
	Herbicide	11.7 ± 2	a 25.2 ± 7.2	ab 0.7	3.88 ± a
	Integrated	10.4 ± 2	ab 25.5 ± 7.8	a 0.7	3.92 ± a
	Mechanical	9.7 ± 2.3	b 19.8 ± 8.1	c 0.7	3.57 ± b

4.2. Weed control strategy affects tree structure

Plots exposed to the integrated and herbicide-based weed control treatments exhibited larger tree geometries, while the trees of the plots that underwent the mechanical and cover crop treatments generally had smaller geometries. The results suggest that the weed-free area adjacent to the tree trunks contributed to tree development due to the inherited reduction of competition with weeds (Brunharo et al., 2020). This point is particularly true for this study as it was held in a young (3-year-old) orchard at the early stages of tree development, resulting in a more pronounced impact on tree development. Judging from the weed cover throughout the years, it is clear that weed cover is most affected (and steady throughout the year) by herbicide treatment, particularly in the cover crop treatment where weed growth is replaced or even promoted. In this respect, weed covers seem to follow natural highs in the winter and merge at low coverage in the summer, and it doesn't seem to be well correlated to tree size. The different weed control approaches have a complex trade-off between their efficiency vs. crop development and long-term environmental implications (Aggelopoulou et al., 2011; Hocevar et al., 2014). It is now accepted that herbicides negatively affect non-target organisms and pollute groundwater with unwanted, often toxic deposits that slowly creep into the food supply, causing the accumulation of toxins in mammals (Bajwa et al., 2015). Moreover, while herbicides are a widespread, cost-effective, and efficient way to control weeds, evolutionarily driven herbicide resistance, which neutralizes herbicide effectiveness, is becoming more common (Heap and Duke, 2018). This scenario dictates the need to develop new or integrated weed control approaches that can reduce the reliance on and use of herbicides while minimizing the environmental effect. In the case presented here, the weed control results of integrated treatment were as good as those obtained for the treatment with herbicide alone but at a reduction of 75 % in the amount of herbicide used.

Previous studies suggest that tree TD and yield are correlated, implying that TD reasonably predicts fruit tree yield (Caillaud et al., 2010; Miller and Dietz, 2004; Zuidema, 2003). The correlation between

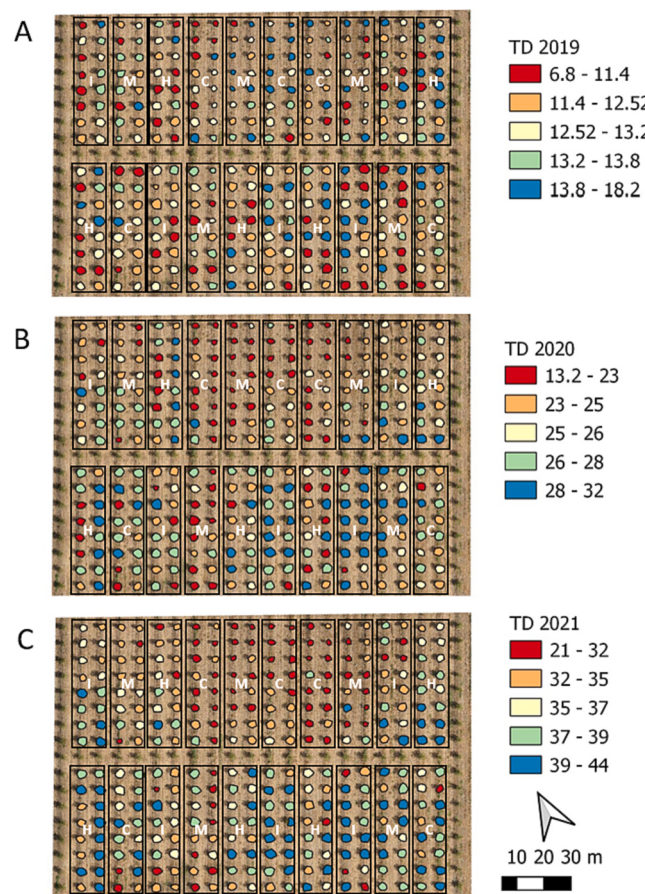


Fig. 8. The individual trunk diameter (TD in cm) measurements for three years (2019–2021; A-C). The spatial distribution of TD values in 2019 differs significantly from that observed in the subsequent years (2020 and 2021), indicating potential changes in tree growth or dynamics over the study period. The scale in values ranges from low (red) to high (blue). The white letter represents the treatment: I - Integrated, M - Mechanical, H - Herbicides, and C - Cover Crop. (For interpretation of the references to color in this figure legend, the reader is referred to the web version of this article.)

GFP and TD may offer an efficient way of achieving similar predictions without the time-consuming, labor-intensive task of TD surveying (e.g., Miller and Dietz, 2004; Rosell and Sanz, 2012; Sarron et al., 2018; Underwood et al., 2016). GFP, as well as the indices for canopy complexity (VCI), for example, can link functionality to yield prediction (e.g., Jin et al., 2020; Zarate-Valdez et al., 2015; Zhang et al., 2019). It should be mentioned, however, that the current experiment investigated relatively young trees and their first harvest (the orchard already bore fruit in 2020 but not harvested). For fruit trees of this age, yield size is not stable, and the correlation between tree size and crop production is not expected to be reliable. The suggested approach should be revisited on older trees to confirm its robustness.

4.3. Structural, temporal, and spatial variability

The bird's-eye view of the orchard suggests an underlying spatial trend in tree geometry parameters. Tree volume, GFP, and TD values showed a generally increasing trend along a southeast-to-northwest axis, and tree height was highest in the eastern part of the orchard. The soil of the orchard itself was relatively uniform, but in terms of its physical parameters, such as slope (slight upward slope from north to south and east to west) and steepness, there was a clear gradient (Figure S.1). Before running the RF partial contribution for tree size spatial distribution, slope, and aspect were found to be correlated to "distance from

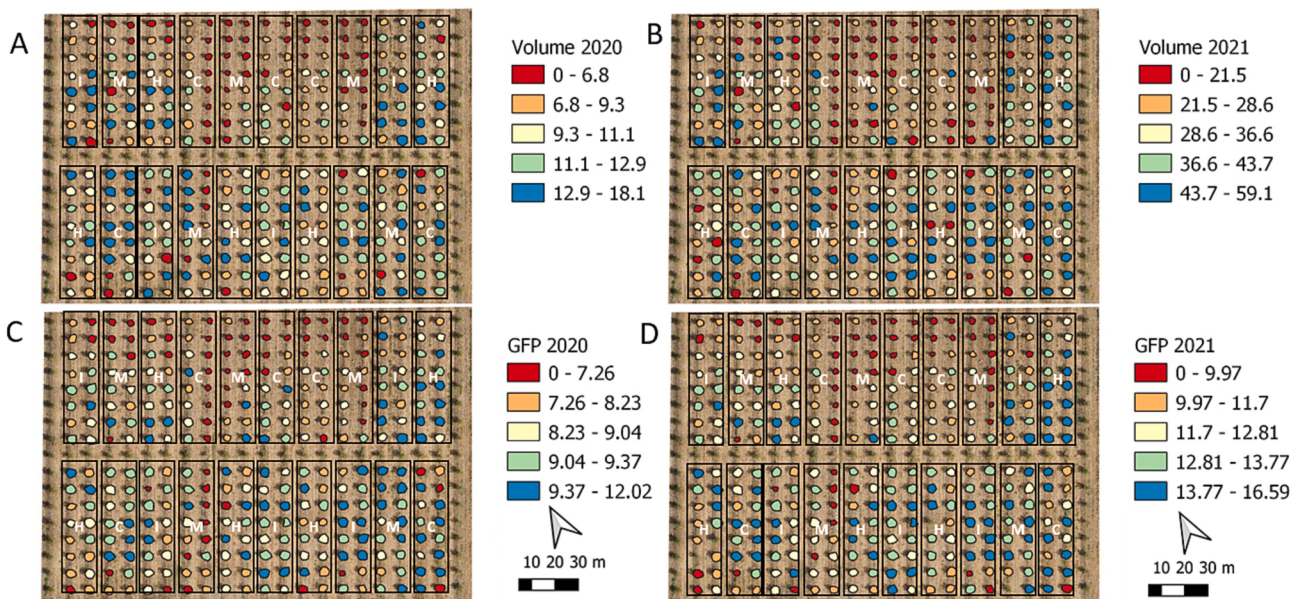


Fig. 9. Individual measurements of tree volume (m^3) and canopy gap fraction (GFP) for the years 2020 and 2021 (A-D). Each map utilizes a different color scale to represent the spatial variation of the corresponding tree structure attribute on the scale from low (red) to high (blue). The white letter represents the treatment: I - Integrated, M – Mechanical, H – Herbicides and C – Cover Crop. (For interpretation of the references to color in this figure legend, the reader is referred to the web version of this article.)

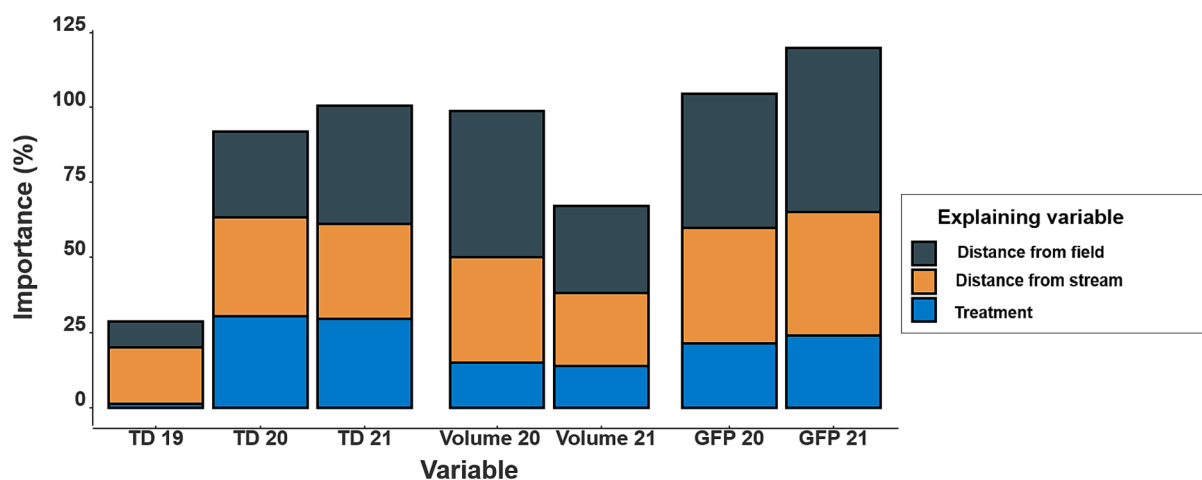


Fig. 10. The relative influence of weed control strategies treatment and environmental variables on three canopy parameters: Canopy Gap Fraction (GFP), Trunk Diameter (TD), and Tree Volume, for the years 2020 and 2021 based on the Random Forest model. The affecting factors – distance from the field, distance from the stream, and IWM treatment are in color.

stream” and were removed from further analysis to avoid multi-collinearity. Therefore, distance from the stream combines and represents all aspects of morphology and natural hydrology for the study plot. While we can speculate that the above may influence water availability and microclimate, the distance to the nearest field effect remains unknown. In addition, from an analytical perspective, the finding that orchard tree geometries are not uniform across the orchard despite the apparent homogenous starting point could also indicate an oversight on the part of the orchard management team. Moreover, remote sensing, in this case, has the merit of enabling the management team to monitor single trees in the orchard without assuming plot uniformity.

4.4. Uncertainties and future work

LiDAR holds significant promise for bridging the gap between tree structural traits and yield prediction. This technology has the potential

to offer a reliable connection between these domains. Future efforts should focus on refining the current algorithms associated with tree geometries (e.g., Brodu and Lague, 2012) and functional algorithms, like alternative GFP calculation methods (Tian et al., 2021). One limitation of the UAV-LiDAR is the sensors’ point density and the field of view, which limits the detection of parameters such as TD and distinguishing between leaves and branches. Previous efforts have combined UAVs with terrestrial LiDAR, with the latter being employed to approximate trunk and undergrowth parameters. This approach offers an alternative to manual TD measurements and delivers a more nuanced canopy profile. An additional promising avenue is to enhance the capabilities of point cloud tree geometry algorithms through spatial fusion of UAV-derived spectral (multispectral or hyperspectral) and thermal data. Moreover, other often-overlooked LiDAR data, such as the number of returns and intensity, warrant further exploration. For instance, the number of returns and the return number can shed light on the fraction

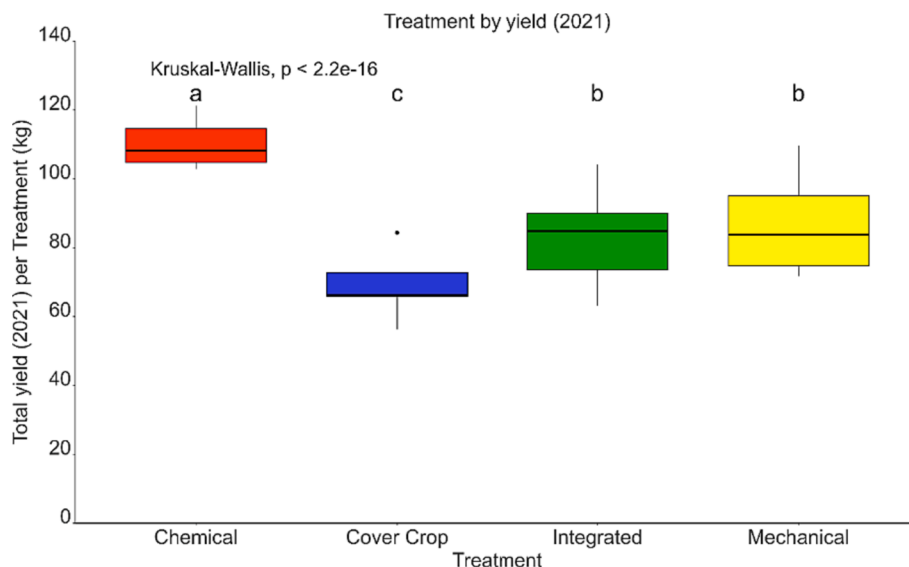


Fig. 11. Plot of yield per experimental treatment for the year 2021. Yield was collected per plot, and the Figure represents the total weight per plot. Letters represent treatment significant differences.

of laser beams absorbed before reaching the ground, thereby providing insights into leaf density through gap fraction Tian et al. (2021). When combined with point intensity values, this information can aid in advanced classification tasks (distinguishing between trunk, branch, or leaf) or nuanced structural analytics like determining leaf surface angles, as highlighted in studies by (Asner et al., 2015; Hill et al., 1987; Torres-Sánchez et al., 2018; Underwood et al., 2016).

Utilizing UAV-LiDAR point cloud data for analyzing tree structure has multiple advantages and limitations. The benefits include high-resolution data that can capture minute details in tree structure, helping detect fine-scale structural differences between trees or within the canopy of individual trees. The point cloud data offers a 3D visualization of the trees, allowing for a comprehensive structural analysis from TCH to understory layers. UAVs can be deployed flexibly based on research requirements, be it a particular time of the day, specific weather conditions, or certain phenological stages. Compared to manned airborne or satellite LiDAR systems, UAV-LiDAR is often more cost-effective for smaller study areas. Finally, the UAV systems allow for repeat measurements over short intervals, which can be critical in studying dynamic changes in tree structure or growth.

However, several limitations need to be addressed as well. Due to battery life and operational constraints, UAVs might not be suitable for very large study areas in a single flight, which, in our case study, wasn't a limitation due to the relatively small size plot. The number of flights with high-resolution data means that data storage, processing, and analysis can require significant computational resources. In addition, there is a learning curve associated with operating UAVs and processing LiDAR data. This may require specialized training to ensure consistent, high-quality data collection. Moreover, in the current study, we worked with a young orchard, but in very dense and developed trees, the penetration capability of LiDAR might be limited, which can affect the reliability of the data related to understory vegetation or lower parts of the tree. Finally, as we showed in our study, proper calibration of the LiDAR system and validation of the data, particularly in complex canopies, can be challenging and require ground-truth data. The accuracy limitation is sometimes related to ground-truth data and sometimes to the LiDAR data.

5. Conclusion

The study described here used UAV-LiDAR point clouds of almond orchards for two consecutive years to quantify the effects of exploiting

different IWM methods on young tree architecture. The LiDAR workflow segmented the almond trees and characterized each tree's geometric features: canopy cover, height, entropy, VCI, volume, and GFP. The described framework for point cloud generation and analysis can accurately detect individual trees, even with some crown overlap. Here, we suggest that almond tree architectures and geometric features provide the information needed to address individual tree needs at the site and at tree-specific scales based on their unique parameters. Our results show a weed control alternative that aligns with the increased interest in using non-chemical weed control and the high public awareness of the damage caused by herbicide misuse. In the case of the almond orchard, it is likely that, as the trees grow in size in the next few years, their sensitivity to weeds and cover crops might have a smaller effect on tree geometries and yield. Furthermore, operational improvements in light of the accumulated experience with weed control alternatives (e.g., the timing and methodology for using cover crops) will improve the results of all non-chemical treatments. The trade-offs, however, are orchard-specific and must be carefully considered. Indeed, that information could help discriminate growth trends, detect and address trees with insufficient vegetative growth, and study their spatial variability. Future work could pursue the fusion of LiDAR data with spectral information to color point clouds, which could add necessary physiological and phenological details on tree status to support better seasonal monitoring. The suggested approach of closely monitoring tree architectures in fruit crop orchards could reduce operating costs (e.g., pesticide application and weed management) and improve overall orchard sustainability by effectively directing its management, such as determining times to harvest, executing mechanized pruning and other relevant agricultural tasks.

Code availability

Not applicable.

CRediT authorship contribution statement

Tamir Caras: Conceptualization, Methodology, Investigation, Data curation, Resources, Writing – original draft, Resources, Writing – review & editing, Visualization. **Ran Nisim Lati:** Conceptualization, Methodology, Investigation, Resources, Data curation, Writing – review & editing, Visualization, Funding acquisition. **Doron Holland:** Investigation, Data curation, Resources, Writing – review & editing. **Vladislav Moshe Dubinin:** Data curation, Resources. **Kamel Hatib:** Data curation. **Itay Shulner:** Data curation. **Ohaliav Keiesar:** Data curation. **Guy**

Liddor: Data curation. **Tarin Paz-Kagan:** Conceptualization, Methodology, Investigation, Resources, Writing – original draft, Resources, Writing – review & editing, Visualization, Funding acquisition.

Declaration of competing interest

The authors declare that they have no known competing financial interests or personal relationships that could have appeared to influence the work reported in this paper.

Data availability

Data will be made available on request.

Appendix A. Supplementary data

Supplementary data to this article can be found online at <https://doi.org/10.1016/j.compag.2023.108467>.

References

- Aggelopoulos, A.D., Bochtis, D., Fountas, S., Swain, K.C., Gemtos, T.A., Nanos, G.D., 2011. Yield prediction in apple orchards based on image processing. *Precis. Agric.* 12, 448–456. <https://doi.org/10.1007/s11119-010-9187-0>.
- Ai, F.-F., Bin, J., Zhang, Z.-M., Huang, J.-H., Wang, J.-B., Liang, Y.-Z., Ling, Y., Yang, Z.-Y., 2014. Application of random forests to select premium quality vegetable oils by their fatty acid composition. *Food chemistry* 143, 472–478.
- Asner, G.P., Hicke, J.A., Lobell, D.B., 2003. Per-pixel analysis of forest structure: Vegetation Indices. Spectral Mixture Anal. Canopy Reflectance Model.
- Asner, G.P., Martin, R.E., Anderson, C.B., Knapp, D.E., 2015. Quantifying forest canopy traits: Imaging spectroscopy versus field survey. *Remote Sens. Environ.* 158, 15–27. <https://doi.org/10.1016/j.rse.2014.11.011>.
- Bajwa, A.A., Mahajan, G., Chauhan, B.S., 2015. Nonconventional Weed Management Strategies for Modern Agriculture. *Weed Sci.* 63, 723–747. <https://doi.org/10.1614/ws-d-15-00064.1>.
- Belding, R.D., Majek, B.A., Lokaj, G.R.W., Hammerstedt, J., Ayeni, A.O., 2004. Orchard Floor Management Influence on Summer Annual Weeds and Young Peach Tree Performance. *Weed Technol.* 18, 215–222. <https://doi.org/10.1614/wt02-180>.
- Bellvert, J., Nieto, H., Pelechá, A., Jofre-Čekalović, C., Zazurca, L., Miarnau, X., 2021. Remote Sensing Energy Balance Model for the Assessment of Crop Evapotranspiration and Water Status in an Almond Rootstock Collection. *Front. Plant Sci.* 12 <https://doi.org/10.3389/fpls.2021.608967>.
- Beniston, J.W., Lal, R., Mercer, K.L., 2016. Assessing and Managing Soil Quality for Urban Agriculture in a Degraded Vacant Lot Soil. *L. Degrad. Dev.* 27, 996–1006. <https://doi.org/10.1002/lqr.2342>.
- Bond, W., Grundy, A.C., 2001. Non-chemical weed management in organic farming systems. *Weed Res.* 41, 383–405. <https://doi.org/10.1046/j.1365-3180.2001.00246.x>.
- Bouvier, M., Durrieu, S., Fournier, R., Renaud, J.-P., 2015. Generalizing predictive models of forest inventory attributes using an area-based approach with airborne LiDAR data. *Remote Sens. Environ.* 156, 322–334. <https://doi.org/10.1016/j.rse.2014.10.004>.
- Brede, B., Lau, A., Bartholomeus, H.M., Kooistra, L., 2017. Comparing RIEGL RiCOPTER UAV LiDAR derived canopy height and DBH with terrestrial LiDAR. *Sensors (Switzerland)* 17, 1–16. <https://doi.org/10.3390/s17102371>.
- Brodt, N., Lague, D., 2012. 3D terrestrial lidar data classification of complex natural scenes using a multi-scale dimensionality criterion: Applications in geomorphology. *ISPRS J. Photogramm. Remote Sens.* 68, 121–134. <https://doi.org/10.1016/j.isprsjprs.2012.01.006>.
- Brunharo, C.A.C.G., Watkins, S., Hanson, B.D., 2020. Season-long weed control with sequential herbicide programs in California tree nut crops. *Weed Technol.* 34, 834–842. <https://doi.org/10.1017/wet.2020.70>.
- Burt, A., Disney, M., Calders, K., 2019. Extracting individual trees from lidar point clouds using treeseg. *Methods Ecol. Evol.* 10, 438–445. <https://doi.org/10.1111/2041-210X.13121>.
- Caillaud, D., Crofoot, M., Scarpino, S., Jansen, P., Garzón López, C.X., Winkelhagen, A., Bohlman, S., Walsh, P., 2010. Modeling the Spatial Distribution and Fruiting Pattern of a Key Tree Species in a Neotropical Forest: Methodology and Potential Applications. *PLoS One* 5, e15002.
- Casanova-Gascón, J., Figueras-Panillo, M., Iglesias-Castellarnau, I., Martín-Ramos, P., 2019. Comparison of SHD and Open-Center Training Systems in Almond Tree Orchards cv. 'soleta'. *Agronomy*. <https://doi.org/10.3390/agronomy9120874>.
- Ewijk, K.Y.V., Treitz, P.M., Scott, N.A., 2011. Characterizing Forest Succession in Central Ontario using Lidar-derived Indices. *Photogramm. Eng. Remote Sensing* 77, 261–269. <https://doi.org/10.14358/PERS.77.3.261>.
- Fan, G., Nan, L., Chen, F., Dong, Y., Wang, Z., Li, H., Chen, D., 2020. A New Quantitative Approach to Tree Attributes Estimation Based on LiDAR Point Clouds. *Remote Sens.* <https://doi.org/10.3390/rs12111779>.
- Fennimore, S.A., Doohan, D.J., 2008. The Challenges of Specialty Crop Weed Control. Future Directions. *Weed Technol.* 22, 364–372. <https://doi.org/10.1614/wt-07-102.1>.
- Gao, S., Zhang, Z., Cao, L., 2021. Individual Tree Structural Parameter Extraction and Volume Table Creation Based on Near-Field LiDAR Data: A Case Study in a Subtropical Planted Forest. *Sensors*. <https://doi.org/10.3390/s21238162>.
- Gianessi, L.P., Reigner, N.P., 2007. The Value of Herbicides in U.S. Crop Production. *Weed Technol.* 21, 559–566. <https://doi.org/10.1614/wt-06-130.1>.
- Granatstein, D., Wiman, M., Kirby, E., Mullinix, K., 2010. Sustainability trade-offs in organic orchard floor management. *Acta Hortic.* 873, 115–122. <https://doi.org/10.17660/ActaHortic.2010.873.11>.
- Guerra, B., Steenwerth, K., 2012. Influence of Floor Management Technique on Grapevine Growth, Disease Pressure, and Juice and Wine Composition: A Review. *Am. J. Enol. Vitic.* 63, 149 LP – 164. <https://doi.org/10.5344/ajev.2011.10001>.
- Heap, I., Duke, S.O., 2018. Overview of glyphosate-resistant weeds worldwide. *Pest Manag. Sci.* 74, 1040–1049. <https://doi.org/10.1002/ps.4760>.
- Hill, S.J., Stephenson, D.W., Taylor, B.K., 1987. Almond yield in relation to tree size. *Sci. Hortic. (amsterdam)* 33, 97–111. [https://doi.org/10.1016/0304-4238\(87\)90036-7](https://doi.org/10.1016/0304-4238(87)90036-7).
- Hočvar, M., Širok, B., Godesá, T., Stopar, M., 2014. Flowering estimation in apple orchards by image analysis. *Precis. Agric.* 15, 466–478.
- Holland, D., Bar-Ya'akov, I., Hatib, K., Birger, R., 2016. 'Matan', a New Self-compatible Almond Cultivar with High-quality Kernel and Good Yield. *HortSci.* 51, 302–304. <https://doi.org/10.21273/HORTSCI.51.3.302>.
- Jabran, K., Chauhan, B.S., 2018. Overview and significance of non-chemical weed control. In: Jabran, K., Chauhan, B.-S.-B.-T.-N.-C.-W.-C. (Eds.), *Non-Chemical Weed Control*. Academic Press, pp. 1–8. <https://doi.org/10.1016/B978-0-12-809881-3.00001-2>.
- Janick, J., 2006. *Horticultural Reviews, Volume 32*. Wiley.
- Jarron, L.R., Coops, N.C., MacKenzie, W.H., Tompalski, P., Dykstra, P., 2020. Detection of sub-canopy forest structure using airborne LiDAR. *Remote Sens. Environ.* 244, 111770 <https://doi.org/10.1016/j.rse.2020.111770>.
- Jin, Y., Chen, B., Lampinen, B.D., Brown, P.H., 2020. Advancing Agricultural Production With Machine Learning Analytics: Yield Determinants for California's Almond Orchards. *Front. Plant Sci.* 11 <https://doi.org/10.3389/fpls.2020.00290>.
- Kamoske, A.G., Dahlin, K.M., Stark, S.C., Serbin, S.P., 2019. Leaf area density from airborne LiDAR: Comparing sensors and resolutions in a temperate broadleaf forest ecosystem. *For. Ecol. Manage.* 433, 364–375. <https://doi.org/10.1016/j.foreco.2018.11.017>.
- Kuhn, M., 2008. Building Predictive Models in R Using the caret Package. *J. Stat. Softw.* 28, 1–26. <https://doi.org/10.18637/jss.v028.i05>.
- Latí, R.N., Rosenfeld, L., David, I.B., Bechar, A., 2021. Power on! Low-energy electrophysical treatment is an effective new weed control approach. *Pest Manag. Sci.* 77, 4138–4147. <https://doi.org/10.1002/ps.6451>.
- Lee, K.H., Ehsani, R., 2009. A Laser Scanner Based Measurement System for Quantification Of Citrus Tree Geometric Characteristics. *Appl. Eng. Agric.* 25, 777–788.
- Levi, Nathan, Hillel, Noa, Zaady, Eli, Rotem, Guy, Ziv, Yaron, Karniel, Arnon, Paz-Kagan, Tarin, 2021. Soil quality index for assessing phosphate mining restoration in a hyper-arid environment. *Ecological Indicators* 125, 107571.
- Mechergui, T., Pardos, M., Jhariya, M.K., Banerjee, A., 2021. Mulching and Weed Management Towards Sustainability BT - Ecological Intensification of Natural Resources for Sustainable Agriculture, in: Jhariya, M.K., Meena, R.S., Banerjee, A. (Eds.), Springer Singapore, Singapore, pp. 255–287. https://doi.org/10.1007/978-981-33-4203-3_8.
- Melander, B., Rasmussen, I.A., Bärberi, P., 2005. Integrating physical and cultural methods of weed control—examples from European research. *Weed Sci.* 53, 369–381. <https://doi.org/10.1614/ws-04-136r>.
- Mia, M.J., Massetani, F., Murri, G., Facci, J., Monaci, E., Amadio, L., Neri, D., 2020. Integrated weed management in high density fruit orchards. *Agronomy*. <https://doi.org/10.3390/agronomy1010492>.
- Miller, K.E., Dietz, J.M., 2004. Fruit Yield, not DBH or Fruit Crown Volume, Correlates with Time Spent Feeding on Fruits by Wild *Leontopithecus rosalia*. *Int. J. Primatol.* 25, 27–39. <https://doi.org/10.1023/B:IJOP.0000014643.20674.97>.
- Moretti, M.L., Bobadilla, L.K., Hanson, B.D., 2021. Cross-resistance to diquat in glyphosate/paraquat-resistant hairy fleabane (*Conyza bonariensis*) and horseweed (*Conyza canadensis*) and confirmation of 2,4-D resistance in *Conyza bonariensis*. *Weed Technol.* 35, 554–559. <https://doi.org/10.1017/wet.2021.11>.
- Rodriguez-Galiano, V.F., Chica-Olmo, M., Abarca-Hernandez, F., Atkinson, P.M., Jeganathan, C., 2012. Random Forest classification of Mediterranean land cover using multi-seasonal imagery and multi-seasonal texture. *Remote Sens. Environ.* 121, 93–107. <https://doi.org/10.1016/j.rse.2011.12.003>.
- Rojo, F., Dhillon, R., Upadhyaya, S., Jenkins, B., Lampinen, B., Roach, J., Metcalf, S., 2014. Modeling Canopy Light Interception for Estimating Potential Yield in Almond and Walnut Trees. 2014 Montr. Quebec Canada July 13 – July 16, 2014, ASABE Paper No. 141896144. <https://doi.org/10.13031/aim.20141896144>.
- Rosell, J.R., Sanz, R., 2012. A review of methods and applications of the geometric characterization of tree crops in agricultural activities. *Comput. Electron. Agric.* <https://doi.org/10.1016/j.compag.2011.09.007>.
- Roussel, J.R., Auty, D., Coops, N.C., Tompalski, P., Goodbody, T.R.H., Meador, A.S., Bourdon, J.F., de Boissieu, F., Achim, A., 2020. lidR: An R package for analysis of Airborne Laser Scanning (ALS) data. *Remote Sens. Environ.* 251, 112061 <https://doi.org/10.1016/j.rse.2020.112061>.
- Sarron, J., Malézieux, É., Sané, C.A.B., Faye, É., 2018. Mango Yield Mapping at the Orchard Scale Based on Tree Structure and Land Cover Assessed by UAV. *Remote Sens.* 10 <https://doi.org/10.3390/rs10121900>.

- Sharma, P., 2020. What is Predictive Power Score (PPS) – Is it better than Correlation ? [With Python Code] [WWW Document]. machinelearningknowledge.ai. URL <https://machinelearningknowledge.ai/predictive-power-score-vs-correlation-with-python-implementation/>.
- Silva, C.A., Hudak, A.T., Vierling, L.A., Loudermilk, E.L., O'Brien, J.J., Hiers, J.K., Jack, S.B., Gonzalez-Benecke, C., Lee, H., Falkowski, M.J., Khosravipour, A., 2016. Imputation of Individual Longleaf Pine (*Pinus palustris* Mill.) Tree Attributes from Field and LiDAR Data. *Can. J. Remote Sens.* 42, 554–573. <https://doi.org/10.1080/07038992.2016.1196582>.
- Tian, L., Qu, Y., Qi, J., 2021. Estimation of forest lai using discrete airborne lidar: A review. *Remote Sens.* 13 <https://doi.org/10.3390/rs13122408>.
- Torres-Sánchez, J., de Castro, A.I., Peña, J.M., Jiménez-Brenes, F.M., Arquero, O., Lovera, M., López-Granados, F., 2018. Mapping the 3D structure of almond trees using UAV acquired photogrammetric point clouds and object-based image analysis. *Biosyst. Eng.* 176, 172–184. <https://doi.org/10.1016/j.biosystemseng.2018.10.018>.
- Underwood, J.P., Hung, C., Whelan, B., Sukkarieh, S., 2016. Mapping almond orchard canopy volume, flowers, fruit and yield using lidar and vision sensors. *Comput. Electron. Agric.* 130, 83–96. <https://doi.org/10.1016/j.compag.2016.09.014>.
- Verma, N.K., Lamb, D.W., Reid, N., Wilson, B., 2016. Comparison of canopy volume measurements of scattered eucalypt farm trees derived from high spatial resolution imagery and LiDAR. *Remote Sens.* 8 <https://doi.org/10.3390/rs8050388>.
- West, P., 2009. Tree and forest measurement: 2nd edition, *Tree and Forest Measurement: 2nd Edition*. <https://doi.org/10.1007/978-3-540-95966-3>.
- Westwood, J.H., Charudattan, R., Duke, S.O., Fennimore, S.A., Marrone, P., Slaughter, D.C., Swanton, C., Zollinger, R., 2018. Weed Management in 2050: Perspectives on the Future of Weed Science. *Weed Sci.* 66, 275–285. <https://doi.org/10.1017/wsc.2017.78>.
- Wetschoreck, F., Tobias, K., Krishnamurthy, S., 2020. 8080labs/ppscode: zenodo release. Zenodo. <https://doi.org/10.5281/zenodo.4091345>.
- Wu, D., Phinn, S., Johansen, K., Robson, A., Muir, J., Searle, C., 2018. Estimating changes in leaf area, leaf area density, and vertical leaf area profile for Mango, Avocado, and Macadamia tree crowns using Terrestrial Laser Scanning. *Remote Sens.* 10 <https://doi.org/10.3390/rs10111750>.
- Yang, J., Kang, Z., Cheng, S., Yang, Z., Akwensi, P., 2020. An individual tree segmentation method based on watershed algorithm and 3D spatial distribution analysis from airborne LiDAR point clouds. *IEEE J. Sel. Top. Appl. Earth Obs. Remote Sens.* 13, 1055–1067. <https://doi.org/10.1109/JSTARS.2020.2979369>.
- Yin, D., Wang, L., 2019. Individual mangrove tree measurement using UAV-based LiDAR data: Possibilities and challenges. *Remote Sens. Environ.* 223, 34–49. <https://doi.org/10.1016/j.rse.2018.12.034>.
- Zarate-Valdez, J., Muhammad, S., Saa, S., Lampinen, B., Brown, P., 2015. Light interception, leaf nitrogen and yield prediction in almonds: A case study. *Eur. J. Agron.* 66, 1–7. <https://doi.org/10.1016/j.eja.2015.02.004>.
- Zhang, P., Guo, Z., Ullah, S., Melagraki, G., Afantitis, A., Lynch, I., 2021. Nanotechnology and artificial intelligence to enable sustainable and precision agriculture. *Nat. Plants* 7, 864–876. <https://doi.org/10.1038/s41477-021-00946-6>.
- Zhang, Z., Jin, Y., Chen, B., Brown, P., 2019. California almond yield prediction at the orchard level with a machine learning approach. *Front. Plant Sci.* 10 <https://doi.org/10.3389/fpls.2019.00809>.
- Zhao, T., Doll, D., Wang, D., Chen, Y., 2017. A new framework for UAV-based remote sensing data processing and its application in almond water stress quantification. In: In: 2017 International Conference on Unmanned Aircraft Systems (ICUAS), pp. 1794–1799. <https://doi.org/10.1109/ICUAS.2017.7991498>.
- Zhao, K., Popescu, S., 2020. Lidar-based mapping of leaf area index and its use for validating GLOBCARBON satellite LAI product in a temperate forest of the southern USA. *Remote Sens. Environ.* 240, 1628–1645. <https://doi.org/10.1016/j.rse.2020.111696>.
- Zhu, C., Zhang, X., Hu, B., Jaeger, M., 2008. Reconstruction of tree crown shape from scanned data. *Lect. Notes Comput. Sci. (including Subser. Lect. Notes Artif. Intell. Lect. Notes Bioinformatics)* 5093 LNCS, 745–756. https://doi.org/10.1007/978-3-540-69736-7_79.
- Zhu, Z., Kleinn, C., Nölke, N., 2021. Assessing tree crown volume - A review. *Forestry* 94, 18–35. <https://doi.org/10.1093/forestry/cpaa037>.
- Zhu, X., Liu, J., Skidmore, A.K., Premier, J., Heurich, M., 2020. A voxel matching method for effective leaf area index estimation in temperate deciduous forests from leaf-on and leaf-off airborne LiDAR data. *Remote Sens. Environ.* 240, 111696 <https://doi.org/10.1016/j.rse.2020.111696>.
- Zuidema, P., 2003. Ecology and management of the Brazil nut tree (*Bertholletia excelsa*). *PROMAB Sci. Ser.*